

# The influence of defect states on non-equilibrium carrier dynamics in GaN nanowires

Prashanth C Upadhy<sup>1,3</sup>, Qiming Li<sup>2</sup>, George T Wang<sup>2</sup>,  
Arthur J Fischer<sup>2</sup>, Antoinette J Taylor<sup>1</sup> and Rohit P Prasankumar<sup>1</sup>

<sup>1</sup> Center for Integrated Nanotechnologies, Los Alamos National Laboratory, Los Alamos, NM 87545 USA

<sup>2</sup> Sandia National Laboratories, PO Box 5800, MS-1086, Albuquerque, NM 87185 USA

E-mail: [pupadhy@lanl.gov](mailto:pupadhy@lanl.gov)

Received 21 September 2009, in final form 1 December 2009

Published 22 January 2010

Online at [stacks.iop.org/SST/25/024017](http://stacks.iop.org/SST/25/024017)

## Abstract

Semiconductor nanowires have recently attracted much attention for their unique properties and potential applications in a number of areas, most notably in nanophotonics. However, the presence of defect states in these quasi-one-dimensional nanostructures can significantly detract from nanophotonic device performance. Here, we use ultrafast optical pump-probe spectroscopy to study the influence of defect states on carrier dynamics in GaN nanowires by probing carrier relaxation through the states responsible for yellow luminescence, an undesirable effect that plagues many GaN-based photonic devices. Faster relaxation is seen in nanowires grown at lower temperatures, which also exhibits higher lasing thresholds. We attribute this to rapid trapping of photoexcited carriers into additional impurity sites that are present at lower growth temperatures. In addition, excitation density-dependent measurements reveal a decrease in carrier lifetimes with increasing pump fluence. These results demonstrate the influence of both radiative and non-radiative defect states on carrier dynamics in GaN nanowires and indicate that relaxation rates can be controlled by varying the growth temperature, which should enable researchers to optimize nanowire properties for a given application.

(Some figures in this article are in colour only in the electronic version)

## 1. Introduction

The synthesis and optical characterization of semiconductor nanowires (NWs) has gained considerable attention in recent years [1–7]. These quasi-one-dimensional (1D) nanostructures exhibit unique electronic and optical properties arising from their anisotropic geometry, large surface to volume ratio and two-dimensional quasi-particle confinement, making them promising candidates for a wide range of applications. One of the most intensively studied areas is nanophotonics, which has led to the demonstration of NW-based microcavity lasers, waveguides, photodetectors and light emitting diodes (LEDs) [1, 2, 6, 8]. These exciting developments suggest that NW-based nanophotonic devices

have the potential to overcome current limitations of electronic devices and enable high-speed all-optical communication and computing at the nanoscale [6].

GaN NWs are of great interest in this regard since they emit light in the technologically important ultraviolet–blue spectral range, which has motivated the development of GaN NW-based LEDs [8] and lasers [1, 9, 10]. Furthermore, alloying with indium offers the ability to tune the band gap across the visible, extending the applicability of these nanosystems [7]. However, as in bulk GaN [11], GaN NWs contain structural and point defects that can trap carriers from band-edge states before they can radiatively recombine [12, 13], which will reduce LED efficiencies and raise laser thresholds. In addition, the lifetime of carriers in these defect states will influence the modulation bandwidth of GaN NW-

<sup>3</sup> Author to whom any correspondence should be addressed.

based nanophotonic devices. Further progress in this area will therefore depend on understanding the influence of defect states on ultrafast carrier relaxation in GaN NWs after injection into the conduction and valence bands.

Carrier dynamics in near-band-edge defect states in GaN NWs have previously been examined using time-resolved photoluminescence (TRPL) spectroscopy [14–16]. However, this technique can only directly probe radiative transitions (proportional to the product of electron and hole distributions), with typical time resolution of a few picoseconds (ps). In contrast, ultrafast optical pump-probe spectroscopy is sensitive to the sum of electron and hole distributions and can therefore probe both radiative and non-radiative transitions with femtosecond (fs) time resolution [5], giving deeper insight into individual energy transfer processes that occur on a sub-picosecond time scale. Although the application of this technique to semiconductor nanowires is still relatively unexplored [2–5, 17–21], ultrafast optical experiments that probe defect levels in GaN NWs should provide some insight into the role of these states in carrier relaxation, which will aid in optimizing these nanosystems for device applications.

Here, we focus on one of the most common defects, the broad ‘yellow luminescence (YL)’ band that has been observed in nearly all GaN-based systems [11], including NWs [22, 23]. In the unintentionally n-doped GaN NWs studied here [23], the observed YL emission (and probe absorption) is likely due to a transition between the conduction band minima and acceptor defect states that are located  $\sim 0.8$ – $1.2$  eV above the valence band [11, 24]. While the nature of the defect states responsible for YL is not fully understood, variations in growth conditions, including the substrate temperature ( $G_{\text{sub}}$ ) and III–V precursor ratio, have been found to influence the nature of defect states and change the band-edge luminescence (BEL) [22, 23, 25], providing a means for optimizing the NW optical properties. In this paper, we examine the influence of the growth temperature on carrier relaxation through YL defect states by measuring the time-resolved transmission of a probe laser pulse, with wavelength tuned to the center of the YL band, after above-band-gap excitation in GaN NWs grown at different temperatures. Carrier lifetimes are found to decrease with decreasing growth temperature, attributed to rapid carrier trapping into additional non-radiative defect states that are present at lower growth temperatures. We then correlate the measured ultrafast dynamics with time-integrated PL measurements to further support our interpretation. Finally, we also examine the dependence of relaxation rates on the photoexcited carrier density, studies that are particularly relevant to applications in NW lasing. These results demonstrate that carrier relaxation in GaN NWs is strongly influenced by the presence of both radiative and non-radiative defect states but can be modified through control of the growth temperature, which will be important for future applications of these nanostructures as lasers and LEDs.

## 2. Experimental details

The growth of the GaN NWs used in this study has been described in detail elsewhere [23]. In brief, nanowires

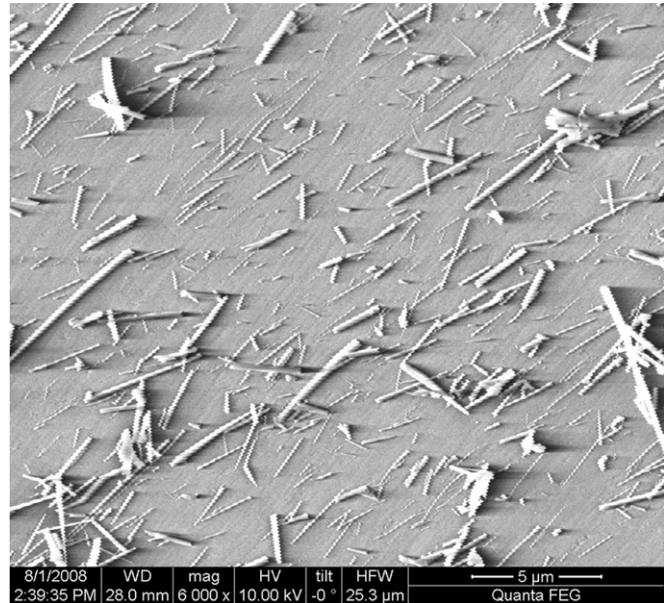


**Figure 1.** SEM image of VLS-grown GaN NWs dry transferred onto a sapphire substrate. Direct optical measurements on as-grown NWs synthesized on *r*-plane sapphire are complicated by a GaN film that grows along with the NWs, making it difficult to extricate carrier dynamics solely due to the NWs from the resulting signal.

were synthesized on (1 $\bar{1}$ 02) oriented sapphire substrates using metal-organic chemical vapor deposition (MOCVD), employing Ni catalyst nanoparticles to initiate the vapor–liquid–solid (VLS) growth process at substrate temperatures,  $G_{\text{sub}}$ , of 800, 850 or 900 °C [23]. Transmission electron microscopy (TEM) analysis indicated that the resulting NWs are single crystalline with wurtzite structure, aligned vertically to the substrate and crystallographically oriented along the (11 $\bar{2}$ 0) direction. For optical measurements, the nanowires were dry transferred onto a clean sapphire substrate to eliminate contributions to the signal from a GaN film that grows concurrently with the NWs. Scanning electron microscopy (SEM) measurements (figure 1) indicate that the NW areal density is typically  $\sim 12 \times 10^5$  NWs mm $^{-2}$ . The NWs typically have a tapered shape, with lengths of 5–10  $\mu$ m and average diameters of 120–160 nm; a small percentage (<5%) of NWs are larger than 300 nm. The size distribution is comparable for NWs grown at different  $G_{\text{sub}}$ . The relatively large diameter of these NWs implies that quantum effects should not influence the measured dynamics, allowing us to use the properties of bulk GaN to interpret our data.

The time-integrated PL measurement uses an  $\sim 800$  ps, 266 nm laser pulse to excite the sample, after which a  $\frac{1}{4}$  m spectrometer disperses the emitted luminescence that is then detected by a liquid nitrogen cooled CCD camera. The ultrafast optical system (figure 2(a)) is based on a 100 kHz regeneratively amplified Ti:sapphire laser producing 50 fs, 10  $\mu$ J pulses at 800 nm (1.55 eV). Half of the power at 800 nm is used to pump an optical parametric amplifier (OPA), while the other half is mixed with residual 400 nm light from the OPA to generate the 266 nm (4.66 eV) pump pulses. The signal wavelength from the OPA is tuned to 550 nm (2.25 eV) to generate the probe pulses. The pump pulse creates

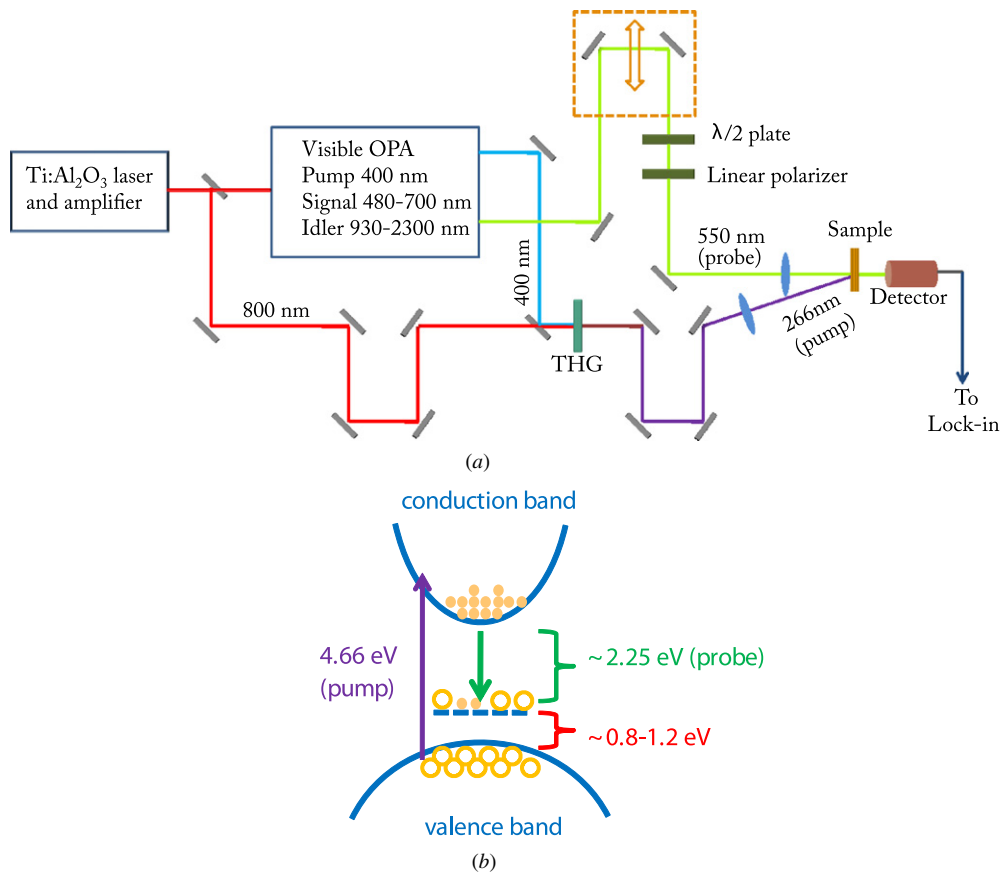


**Figure 2.** (a) Schematic of the setup for UV-pump, visible-probe experiments. (b) Schematic of the energy levels in GaN, depicting the position of the YL-related defect states, related optical transitions, and electron and hole populations after pump excitation.

electron-hole pairs above the band edge in the GaN NWs with a carrier density of  $\sim 7.9 \times 10^{18} \text{ cm}^{-3}$  (at an incident fluence of  $\sim 254 \mu\text{J cm}^{-2}$ ). All experiments were performed at room temperature with the *p*-polarized probe near normal incidence and the *s*-polarized pump at a  $10^\circ$  incidence angle to the plane of the sapphire substrate; the probe fluence at the sample was  $<10\%$  of the pump fluence. In addition, due to non-uniformity in the NW distribution across the sample surface, we performed measurements at several different positions on the sample and averaged the results to ensure consistency in the presented data. Finally, it is worth noting that in these initial experiments, we focused on ultrafast optical studies of NW ensembles, without attempting to align individual NWs with respect to one another. Therefore, polarization-dependent measurements did not show any significant variations between different pump and probe polarizations. However, techniques exist for aligning NWs within an ensemble [26], which will allow us to explore the influence of NW orientation on carrier dynamics in future experiments.

### 3. Results and discussion

Ultraviolet-pump, visible-probe measurements on GaN NWs grown at 800, 850 and 900 °C are shown in figure 3(a). The 266 nm photoexcitation creates electron-hole pairs above the GaN band edge, from which electrons rapidly relax to the conduction band minimum and holes populate mid-gap

defect states (including those responsible for YL) (figure 2(b)). This causes a decrease in the probe absorption through state filling [5], resulting in a positive normalized pump-induced change in probe transmission ( $\Delta T/T$ ) (peak values  $\sim 2-8 \times 10^{-3}$ ) at 550 nm. The rise time of this signal indicates that these states are populated within  $\sim 500$  fs, independent of  $G_{\text{sub}}$  [5]. However, the timescale for carrier relaxation through the YL states (given by the decay of the  $\Delta T/T$  signals) increases with  $G_{\text{sub}}$ . Relaxation time constants, derived from a numerical fit to the data with a triple exponential decay function, show that carriers in each of the samples measured here relax with an initial fast time constant ( $\sim 1-3$  ps) and then with an intermediate time constant ( $\sim 8-26$  ps) followed by a long decay process ( $\tau \gg 1$  ns) that cannot be accurately extracted from our data.

We performed PL experiments on our samples to aid in understanding the observed increase in carrier lifetimes with  $G_{\text{sub}}$ . Low excitation intensity PL measurements (not shown) indicate that the concentration of defects responsible for YL remains unchanged with  $G_{\text{sub}}$ , as evident from the relative intensity invariance of the YL band, while the BEL intensity is an order of magnitude higher for  $G_{\text{sub}} = 900$  °C than at  $G_{\text{sub}} = 800$  °C [22, 23]. These trends, seen here in NW ensembles, were also observed in [22], in which micro-PL experiments were performed on individual NWs that were grown in the same reactor as our samples under similar conditions. In that work, the lower BEL intensity and

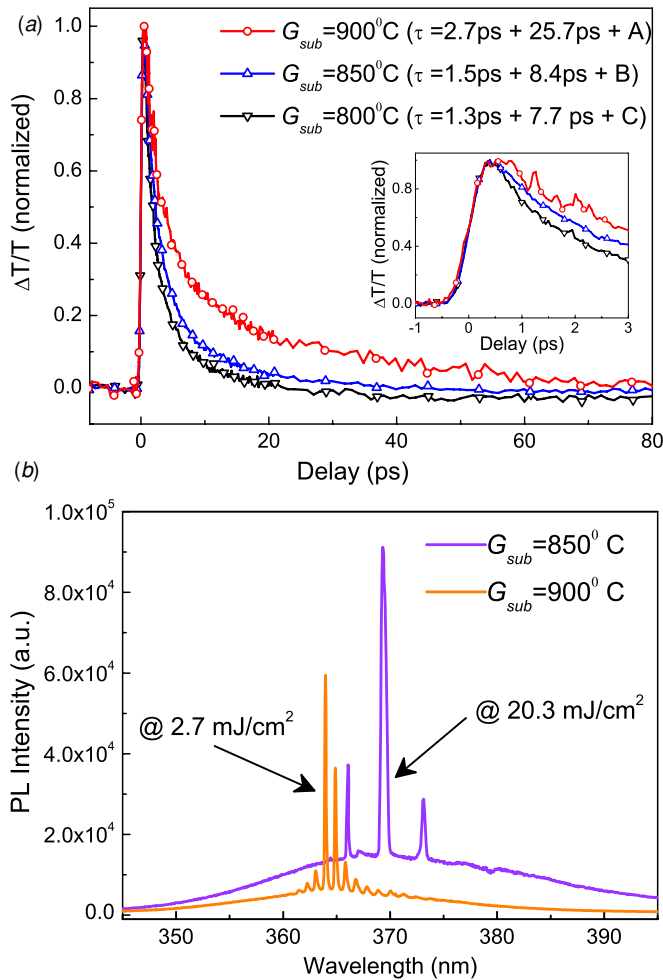


**Figure 3.** (a) UV-pump (266 nm), visible-probe (550 nm) measurements on GaN NWs grown at  $G_{\text{sub}} = 800, 850$  and  $900$  °C. All measurements were performed in transmission at room temperature with a pump fluence of  $254 \mu\text{J cm}^{-2}$ . A triple exponential fits each curve well, and constants A, B and C represent a long relaxation time constant ( $\tau \gg \text{ns}$ ) that cannot be extracted in our experiment. Inset: data plotted for the first 3 ps to focus on the  $G_{\text{sub}}$ -independent rise time. (b) Time-integrated BEL spectra revealing lasing near the threshold for a 266 nm pump. The threshold excitation density is higher for NWs with lower  $G_{\text{sub}}$ , due to the enhanced non-radiative trapping of carriers at defect states. The spectra show Fabry-Perot cavity modes whose average mode spacing varies along the sample surface due to changes in the NW size distribution.

electrical conductivity in NWs with lower  $G_{\text{sub}}$  was attributed to the presence of additional impurity sites in those NWs, possibly due to carbon incorporation from carbon-bearing precursors present during growth, that non-radiatively trap photoexcited carriers [22, 23]. Deep level optical spectroscopy measurements on similar NWs further confirmed the presence of deep level defects in the band gap, and carbon is considered to be a more likely source for some of these defects [12]. This growth temperature-dependent concentration of impurity sites is also likely to be the origin of the differences in BEL intensity between our NW samples grown at different  $G_{\text{sub}}$ . This agrees with previous TRPL measurements on GaN films, which revealed that carrier relaxation was governed by trapping at

impurity sites through non-radiative relaxation processes, thus affecting the time-integrated BEL intensity [27]. In addition, fluence-dependent PL measurements on our samples indicate that these non-radiative defects can also influence NW lasing as shown in figure 3(b)), which reveals a decreased lasing threshold for NWs with higher  $G_{\text{sub}}$  ( $F_{\text{thresh}} \cong 20.3 \text{ mJ cm}^{-2}$  and  $2.7 \text{ mJ cm}^{-2}$  for NWs with  $G_{\text{sub}} = 850$  °C and  $G_{\text{sub}} = 900$  °C, respectively), again likely due to carrier trapping in defect states for NWs grown at low temperatures. Finally, TEM analysis revealed no dislocations for nanowires grown at different  $G_{\text{sub}}$ , although (0001) basal plane stacking faults were commonly observed in these nanowires [22, 23]; this implies that dislocation-related states do not significantly contribute to carrier trapping [22].

The time-integrated PL measurements, as discussed above, indicate that non-radiative defect states, which increase in concentration with decreasing  $G_{\text{sub}}$ , trap carriers from the band edge before they can radiatively recombine. In our pump-probe experiments, the decrease in carrier lifetimes with  $G_{\text{sub}}$  can thus be attributed to rapid capture of electrons from the conduction band and holes from the YL defect states by these impurities. Importantly, unlike in the time-integrated PL measurements, our ultrafast optical experiments can directly measure the rates of these capture processes, which will be important in determining the eventual limits on the modulation bandwidth of GaN NW-based photonic devices. In addition, the ability to tailor the carrier lifetime by varying  $G_{\text{sub}}$  should increase the utility of these NWs in nanophotonic applications.

Pump fluence-dependent measurements reveal that the photoexcited carriers relax more rapidly at higher excitation densities (figure 4(a)), irrespective of growth temperature (figure 4(b)). Several different mechanisms can lead to this behavior. One possible contributor to the observed excitation-density dependent relaxation is laser-induced transformation of gallium vacancy-related complexes. These complexes have been linked to the YL and green luminescence (GL) bands, which are attributed to two charge states of the same defect, presumably a gallium vacancy-oxygen complex ( $\text{V}_{\text{Ga}}\text{O}_{\text{N}}$ ) [24]. Excitation density-dependent PL measurements on GaN epilayers have indicated that at higher densities, the  $\sim 2.2$  eV YL band saturates, transforming into a GL band centered at  $\sim 2.5$  eV [24, 28]. In our experiment, the high excitation fluence may saturate the YL states, resulting in the presence of GL-related defect states that can enhance carrier relaxation out of the YL states [24]. Band-gap renormalization could also influence the observed density-dependent dynamics [5]; however, this is unlikely since this effect is only observed in GaN at densities  $> 10^{19} \text{ cm}^{-3}$  [29], which is higher than the maximum photoexcited carrier density in our experiments. This is further confirmed by the spectral invariance of the intensity dependent BEL measurements.

Bimolecular and Auger recombination have also been shown to strongly influence carrier dynamics in CdSe NWs [19]; the latter process, in particular, is strongly dependent on the carrier density and is more significant in nanostructures [5] (as compared to the bulk material) since the spatial confinement increases Coulomb carrier-carrier interactions. Analysis of our fluence-dependent data



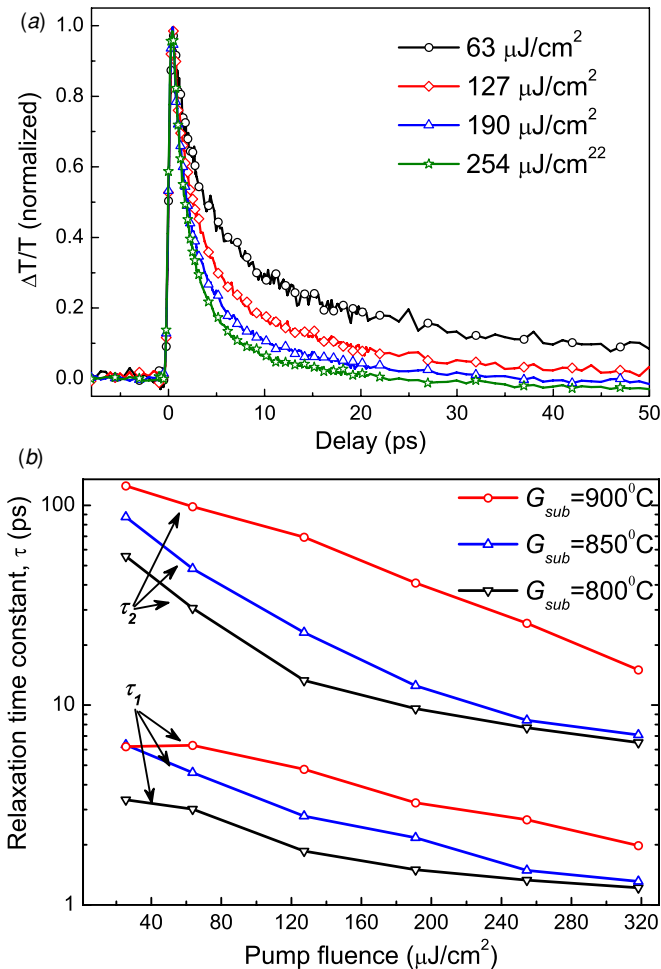


**Figure 4.** (a) Pump fluence-dependent carrier relaxation in NWs grown at  $G_{\text{sub}} = 800^\circ\text{C}$ . (b) Fluence-dependent relaxation time constants in GaN NWs grown at three different temperatures.  $\tau_1$  and  $\tau_2$  are the fast and slow relaxation time constants, respectively, obtained from curve fits.

suggests that bimolecular recombination plays a role at lower fluences, after which Auger recombination takes over at higher fluences, but a more quantitative account of fluence-dependent dynamics in our GaN NWs cannot be given due to the wide size distribution and lack of highly aligned NWs. Further studies will be required to conclusively determine the relative contributions of these mechanisms to the observed fluence-dependent relaxation. Finally, to the best of our knowledge, these are the first ultrafast optical measurements that probe YL defect states in any GaN material (not only NWs), and therefore the insight gained from these measurements may also apply to bulk and thin film GaN.

#### 4. Conclusions

In summary, time-resolved optical spectroscopy was performed on GaN NWs synthesized under different growth conditions. Measurements of carrier relaxation through the defect states responsible for yellow luminescence in NWs with different  $G_{\text{sub}}$  indicate that the growth temperature is an effective way to minimize the role of additional defect states

in carrier relaxation. Excitation-density-dependent changes in carrier lifetimes are likely due to many-body interactions, with a potential contribution from relaxation through additional laser-induced defect states. Our experiments thus demonstrate the value of ultrafast optical spectroscopy in understanding the nature of defect states in semiconductor NWs, while suggesting approaches toward controlling or minimizing their influence on carrier relaxation dynamics and thereby optimizing NW-based devices for nanophotonic applications. Furthermore, we expect ultrafast optical measurements on single GaN NWs to be possible in the near future, which will be a powerful approach for studying non-equilibrium carrier dynamics in these nanosystems without the influence of ensemble broadening.

#### Acknowledgments

This work was performed at the Center for Integrated Nanotechnologies, a US Department of Energy, Office of Basic Energy Sciences (BES) user facility and also partially supported by the NNSA's Laboratory Directed Research and Development Program and the Department of Energy, Office of Basic Energy Sciences. Los Alamos National Laboratory, an affirmative action equal opportunity employer, is operated by Los Alamos National Security, LLC, for the National Nuclear Security administration of the U.S. Department of Energy under contract no. DE-AC52-06NA25396. Sandia is a multiprogram laboratory operated by Sandia Corporation, a Lockheed Martin Company, for the United States Department of Energy's National Nuclear Security Administration under contract no. DE-AC04-94AI85000.

#### References

- [1] Johnson J C, Choi H J, Knutsen K P, Schaller R D, Yang P and Saykally R J 2002 Single gallium nitride nanowire lasers *Nat. Mater.* **1** 106–10
- [2] Johnson J C, Knutsen K P, Yan H, Law M, Zhang Y, Yang P and Saykally R J 2004 Ultrafast carrier dynamics in single ZnO nanowire and nanoribbon lasers *Nano Lett.* **4** 197–204
- [3] Parkinson P, Lloyd-Hughes J, Gao Q, Tan H H, Jagadish C, Johnston M B and Herz L M 2007 Transient terahertz conductivity of GaAs nanowires *Nano Lett.* **7** 2162–5
- [4] Prasankumar R P, Choi S, Trugman S A, Picraux S T and Taylor A J 2008 Ultrafast electron and hole dynamics in germanium nanowires *Nano Lett.* **8** 1619–24
- [5] Prasankumar R P, Upadhyaya P C and Taylor A J 2009 Ultrafast carrier dynamics in semiconductor nanowires *Phys. Status Solidi B* **246** 1973–95
- [6] Sirbully D J, Law M, Yan H and Yang P 2005 Semiconductor nanowires for subwavelength photonics integration *J. Phys. Chem. B* **109** 15190–213
- [7] Yang P 2005 The chemistry and physics of semiconductor nanowires *Mater. Res. Soc. Bull.* **30** 85–91
- [8] Zhong Z, Qian F, Wang D and Lieber C M 2003 Synthesis of p-type gallium nitride nanowires for electronic and photonic nanodevices *Nano Lett.* **3** 343–6
- [9] Gradecek S, Qian F, Li Y, Park H-G and Lieber C M 2005 GaN nanowire lasers with low lasing thresholds *Appl. Phys. Lett.* **87** 173111
- [10] Pauzauskie P J, Sirbully D J and Yang P 2006 Semiconductor nanowire ring resonator laser *Phys. Rev. Lett.* **96** 143903

- [11] Reshchikov M A and Morkoc H 2005 Luminescence properties of defects in GaN *J. Appl. Phys.* **97** 061301
- [12] Armstrong A, Li Q, Bogart K H A, Lin Y, Wang G T and Talin A A 2009 Deep level optical spectroscopy of GaN nanorods *J. Appl. Phys.* **106** 053712
- [13] Armstrong A, Wang G T and Talin A A 2009 Depletion-mode photoconductivity study of deep levels in GaN nanowires *J. Electron. Mater.* **38** 484–9
- [14] Chin A H, Ahn T S, Li H, Vaddiraju S, Bardeen C J, Ning C-Z and Sunkara M K 2007 Photoluminescence of GaN nanowires of different crystallographic orientations *Nano Lett.* **7** 626–31
- [15] Schlager J B, Bertness K A, Blanchard P T, Robins L H, Roshko A and Sanford N A 2008 Steady-state and time-resolved photoluminescence from relaxed and strained GaN nanowires grown by catalyst-free molecular-beam epitaxy *J. Appl. Phys.* **103** 124309–6
- [16] Yoo J, Hong Y-J, An S J, Yi G-C, Chon B, Joo T, Kim J-W and Lee J-S 2006 Photoluminescent characteristics of Ni-catalyzed GaN nanowires *Appl. Phys. Lett.* **89** 043124
- [17] Baxter J B and Schmuttenmaer C A 2006 Conductivity of ZnO nanowires, nanoparticles and thin films using time-resolved terahertz spectroscopy *J. Phys. Chem. B* **110** 25229–39
- [18] Othonos A, Lioudakis E, Philipose U and Ruda H E 2007 Ultrafast carrier dynamics in band edge and broad deep defect emission ZnSe nanowires *Appl. Phys. Lett.* **91** 241113
- [19] Robel I, Bunker B A, Kamat P V and Kuno M 2006 Exciton recombination dynamics in CdSe nanowires: bimolecular to three-carrier Auger kinetics *Nano Lett.* **6** 1344–9
- [20] Othonos A, Zervos M and Pervolaraki M 2008 Ultrafast carrier relaxation in InN nanowires grown by reactive vapor transport *Nanoscale Res. Lett.* **4** 122–9
- [21] Song J K, Willer U, Szarko J M, Leone S R, Li S and Zhao Y 2008 Ultrafast upconversion probing of lasing dynamics in single ZnO nanowire lasers *J. Phys. Chem. C* **112** 1679–84
- [22] Talin A A, Wang G T, Lai E and Anderson R J 2008 Correlation of growth temperature, photoluminescence and resistivity in GaN nanowires *Appl. Phys. Lett.* **92** 093105
- [23] Wang G T, Talin A A, Werder D J, Creighton J R, Lai E, Anderson R J and Arslan I 2006 Highly aligned, template-free growth and characterization of vertical GaN nanowires on sapphire by metal–organic chemical vapour deposition *Nanotechnology* **17** 5773–80
- [24] Reshchikov M A, Morkoc H, Park S S and Lee K Y 2002 Two charge states of dominant acceptor in unintentionally doped GaN: evidence from photoluminescence study *Appl. Phys. Lett.* **81** 4970–2
- [25] Mickevicius J, Aleksiejunas R, Shur M S, Sakalauskas S, Tamulaitis G, Fareed Q and Gaska R 2005 Correlation between yellow luminescence intensity and carrier lifetimes in GaN epilayers *Appl. Phys. Lett.* **86** 041910
- [26] Fan Z, Ho J C, Jacobson Z A, Yerushalmi R, Alley R L, Razavi H and Javey A 2007 Wafer-scale assembly of highly ordered semiconductor nanowire arrays by contact printing *Nano Lett.* **8** 20–5
- [27] Shan W, Xie X C, Song J J and Goldenberg B 1995 Time-resolved exciton luminescence in GaN grown by metalorganic chemical vapor deposition *Appl. Phys. Lett.* **67** 2512–4
- [28] Reshchikov M A, Morkoc H, Park S S and Lee K Y 2001 Yellow and green luminescence in a freestanding GaN template *Appl. Phys. Lett.* **78** 3041–3
- [29] Nagai T, Inagaki T J and Kanemitsu Y 2004 Band-gap renormalization in highly excited GaN *Appl. Phys. Lett.* **84** 1284–6